Structural Engineering and Mechanics, Vol. 5, No. 6 (1997) 679-689
DOI: http://dx.doi.org/10.12989/sem.1997.5.6.679

A comprehensive description for damage of concrete subjected to complex loading

Christian Meyer†

Department of Civil Engineering and Engineering Mechanics, Columbia University in the City of New York, U.S.A.

Xianghe Peng‡

Department of Engineering Mechanics, Chongqing University, China

Abstract. The damage of concrete subjected to multiaxial complex loading involves strong anisotropy due to its highly heterogeneous nature and the geometrically anisotropic characteristic of the microcracks. A comprehensive description of concrete damage is proposed by introducing a fourth-order anisotropic damage tensor. The evolution of damage is assumed to be related to the principal components of the current states of stress and damage. The unilateral effect of damage due to the closure and opening of microcracks is taken into account by introducing projection tensors that are also determined by the current state of stress. The proposed damage model considers the different kinds of damage mechanisms that result in different failure modes and different patterns of microdefects that cause different unilateral effects. This damage model is embedded in a thermomechanically consistent constitutive equation, in which hardening and the triaxial compression caused shear-enhanced compaction can also be taken into account. The validity of the proposed model is verified by comparing theoretical and experimental results of plain and steel fiber reinforced concrete subjected to complex triaxial stress histories.

Key words: concrete; damage; damage mechanics; constitutive equation; verification.

1. Introduction

The nonlinearities of concrete behavior under load are caused by two distinct microstructural changes that take place in the material. One is the permanent deformation of the cement matrix, which is comparable to the slip-type plastic flow encountered in metals. The other one is the development of microcracks and microvoids that are commonly associated with damage accumulation. While the plastic deformations are controlled by local shear stresses, the degradation of elastic properties that accompanies damage accumulation is highly oriented and introduces anisotropy even in an initially isotropic material. Thus, the mechanical properties such as ultimate strength and fatigue life depend strongly on the initiation, growth and coalescence of microcracks. The geometrical anisotropy of microcracks induces highly localized stress fields and anisotropic

† Professor
‡ Professor

material properties, which, in turn, result in anisotropic damage. On the other hand, the closure of microcracks under certain stress states causes partial stiffness recovery. This different response to compression and tension stresses is generally referred to as the unilateral effect, and the mechanics of crack opening and closing has an important effect on the material response to cyclic loads. Also the failure modes are typically complex and depend on the pattern of existing microdefects and the stress history at a given point. For example, when load induces extension, mode I cracking may be predominant, but cracks can also propagate in mode II or III.

The constitutive behavior of concrete subjected to complex loading histories has received considerable attention in recent years, and its significance concerning numerous practical applications is being recognized by the profession (ASCE, 1982; ASCE, 1991). Since the two behavior characteristics mentioned above are relatively independent, it appears logical to base a mathematical formulation on a combination of two different theoretical frameworks: the theory of plasticity is well suited to describe the permanent deformations observed in concrete under both monotonic and cyclic loads, whereas continuum damage mechanics is capable of reproducing the degradation of elastic properties as well as the associated anisotropies that result from damage accumulation under repeated load application.

Reviews of constitutive models of concrete with and without fiber reinforcement can be found in the literature (Peng, *et al.* 1997, Paskova 1994, Fang 1996). Herein, a thermomechanically consistent constitutive theory shall be described. It is an extension of the model originally developed by Fan and Peng (1991), Peng and Ponter (1994). It has been shown (Peng, *et al.* 1996) that this theory includes Chaboche's viscoplastic model (Chaboche 1983), the endochronic constitutive formulation of plasticity (Valanis 1980) and many other constitutive models as special cases (Chaboche 1986, Watanabe and Atluri 1986).

Recently, this theory was used to develop a thermomechanically consistent continuum damage model for concrete (Peng, *et al.* 1997). In this work, a modified damage model for concrete is proposed that is embedded in the framework of the thermomechanically consistent equation. Below, a brief summary of the model will be given. Further details can be found in Peng, *et al.* (1997).

2. Constitutive equations

In the past several years, Fan and Peng (1991), Peng and Ponter (1994) proposed thermomechan-

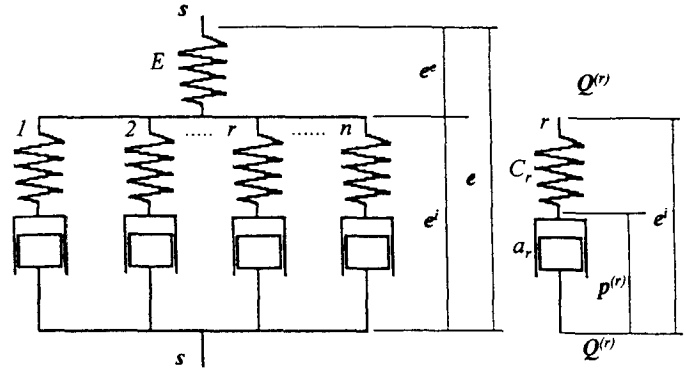

Fig. 1 A simple mechanical model for thermomechanically consistent constitutive equation.

ically consistent constitutive equations for dissipative materials based on a simple mechanical model shown in Fig. 1. It uses n sets of springs C_r (with stiffness $\bar{c}_r$) and dashpot-like blocks a_r (with damping coefficient $\bar{a}_r$) to describe the irreversible behavior of the material, while the elastic response is described by the spring E (with macroscopic shear modulus $\bar{u}$). Assuming concrete is an initially homogeneous and isotropic continuum, and in the case of isothermal and small deformation conditions, one has

$$\boldsymbol{s}=\sum_{r=1}^{n}\boldsymbol{Q}^{(r)},\ \boldsymbol{Q}^{(r)}=\bar{c}_r:(\boldsymbol{e}^i-\boldsymbol{p}^{(r)}) \tag{1}$$

where e^i represents the inelastic deviatoric strain tensor; u is the shear modulus; s is the deviatoric stress tensor; $\boldsymbol{p}^{(r)}$ and $\boldsymbol{Q}^{(r)}$ are the tensors representing, respectively, the rth deviatoric internal variable and the corresponding generalized force that satisfy the following dissipation inequality

$$\boldsymbol{Q}^{(r)}:\frac{d\boldsymbol{p}^{(r)}}{d\zeta_D}\geq 0,\ (r=1,\ 2,\ ...,\ n) \tag{2}$$

in which

$$d\zeta_D{}^2=d\boldsymbol{e}^i:\ d\boldsymbol{e}^i,\ \boldsymbol{Q}^{(r)}=\bar{\boldsymbol{a}}_r:\frac{d\boldsymbol{p}^{(r)}}{d\zeta_D} \tag{3}$$

It is easily seen that ζ_D is non-negative and non-decreasing so that it can be regarded as a generalized time measure, and Eq. (2) is satisfied provided the damping coefficient tensor $\bar{a}_r\ (r=1,\ 2,\ ...,\ n)$ is positive definite. By defining damage as the reduction of load-carrying area (Lemaitre 1987) and noticing the effect of the hydrostatic stress on the mechanical properties and the hardening induced by inelastic deformation, it is reasonable to assume that (Peng, *et al.* 1997)

$$\bar{c}_r=C_r(J_1)\boldsymbol{M},\ \bar{\boldsymbol{a}}_r=f_D\ a_r(J_1)\boldsymbol{M} \tag{4}$$

where $\boldsymbol{M}$ is the fourth-order damage effect tensor, f_D a hardening function, C_r and a_r are material parameters for the undamaged and nonhardening state and J_1 the first invariant of a stress tensor. Combining Eqs. (3), (4) and the differential of Eq. (2), one obtains

$$d\boldsymbol{Q}^{(r)}=C_r\ \boldsymbol{M}:\ d\boldsymbol{e}^i-\alpha_r\boldsymbol{Q}^{(r)}dz_D+d\boldsymbol{M}:\ \boldsymbol{M}^{-1}:\ \boldsymbol{Q}^{(r)}+C_r^{-1}\frac{dC_r}{dJ_1}\,dJ_1\ \boldsymbol{Q}^{(r)} \tag{5}$$

where

$$\alpha_r=\alpha_r(J_1)=\frac{C_r(J_1)}{a_r(J_1)},\qquad dz_D=\frac{d\zeta_D}{f_D} \tag{6}$$

The elastic response can also be obtained from Fig. (1) as

$$\boldsymbol{s}=2\bar{\boldsymbol{u}}:(\boldsymbol{e}-\boldsymbol{e}^i)=2u\boldsymbol{M}:\ (\boldsymbol{e}-\boldsymbol{e}^i) \tag{7}$$

in which e^e and e are elastic and total deviatoric strain, respectively.

Following the procedure similar to that to obtain the deviatoric response, the volumetric component of the response can be obtained as

$$\sigma_{kk}=\sum_{r=1}^{m}\sigma_{kk}{}^{(r)} \tag{8}$$

$$d\sigma_{kk}^{(r)}=E_r M_H d\varepsilon_{kk}^{\ i}-\alpha_H^{(r)}\sigma_{kk}^{(r)}dz_H+dM_H M_H^{-1}\sigma_{kk}^{(r)} \tag{9}$$

in which $\varepsilon_{kk}^{\ i}$ denotes inelastic volumetric strain; M_H is a volumetric damage variable; dz_H is defined in terms of $d\varepsilon^i{}_{kk}$ and hardening function f_H' as follows

$$dz_H=\frac{d\zeta_H}{f_H'}, \quad d\zeta_H=|d\varepsilon^i{}_{kk}| \tag{10}$$

If we choose

$$\left(\frac{1}{f_H'}\right)^2=\left(\frac{1}{f_{DH}}\ \frac{d\zeta_D}{d\zeta_H}\right)^2+\left(\frac{1}{f_H}\right)^2 \tag{11}$$

the effect of deviatoric inelastic deformation on the volumetric response can be taken into account. In Eq. (11), f_H is the volumetric hardening function and f_{DH} a coupling parameter. If f_{DH} is very large the deviatoric inelastic deformation will not markedly affect the volumetric response, otherwise the development of any deviatoric deformation will cause volumetric deformation. The elastic volumetric response can be expressed as

$$\sigma_{kk}=3KM_H(\varepsilon_{kk}-\varepsilon_{kk}^{\ i}) \tag{12}$$

Combining Eqs. (1), (5) and (7) yields the following elastoplastic constitutive equation

$$d\boldsymbol{s}=\left(1+\frac{C}{2u}\right)^{-1}(C\boldsymbol{M}:\ d\boldsymbol{e}+\frac{C}{2u}\,d\boldsymbol{M}:\ \boldsymbol{M}^{-1}:\ \boldsymbol{s}+d\boldsymbol{H}) \tag{13}$$

where

$$C=\sum_{r=1}^{n} C_r,\ d\boldsymbol{H}=\sum_{r=1}^{n}(-\alpha_r\ dz_D\boldsymbol{I}_4+d\boldsymbol{M}:\ \boldsymbol{M}^{-1}+\frac{1}{C_r}\ \frac{dC_r}{dJ_1}\ dJ_1\boldsymbol{I}_4):\ \boldsymbol{Q}^{(r)} \tag{14}$$

Similarly one can obtain the following relation by combining Eqs. (8), (11) and (12)

$$d\sigma_{kk}=\left(1+\frac{G}{3K}\right)^{-1}(GM_H d\varepsilon_{kk}+\frac{G}{3K}\,dM_H M_H^{-1}\sigma_{kk}+dH) \tag{15}$$

in which

$$G=\sum_{r=1}^{m} E_r,\ dH=\sum_{r=1}^{m}[-\alpha_H{}^r\sigma_{kk}dz_H+dM_H M_H^{-1}\sigma_{kk}] \tag{16}$$

3. Damage variables and evolution

With assumptions introduced by Peng, *et al.* (1997), the damage evolution can be expressed as

$$d\boldsymbol{D}=f_1(\sigma,\ \boldsymbol{D})\ dz_D+f_2(\sigma,\ \boldsymbol{D})\ dz_H \tag{17}$$

and the direction of which is assumed to be related to that of the current state of actual stress, i.e.,

$$d\boldsymbol{D}=\sum_{k=1}^{3} dD_k\ \boldsymbol{n}^{(k)}\otimes\boldsymbol{n}^{(k)} \tag{18}$$

where $\boldsymbol{n}(k)$ $(k=1, 2, 3)$ is the eigenvector of the actual stress $\boldsymbol{s}$. Further, in order to embed this damage tensor into the constitutive framework, the following fourth-order damage tensor is defined

$$D_{ijkl}(\boldsymbol{D})=\frac{1}{4}\ (\delta_{ik}D_{jl}+\delta_{jk}D_{il}+\delta_{il}D_{jk}+\delta_{jl}D_{ik}) \tag{19}$$

If the unilateral effect is ignored, then the fourth-order damage effect tensor $\boldsymbol{M}$ can be defined as

$$\boldsymbol{M}=\boldsymbol{I}_4-\boldsymbol{D},\ \text{or}\ M_{ijkl}=I_{ijkl}-D_{ijkl} \tag{20}$$

where I_4 denotes the fourth-order identity tensor. M_H can be derived by combining Eqs. (12) and (19) without considering the unilateral effect:

$$M_H=1-D_I=1-\frac{1}{3}tr(\boldsymbol{D}) \tag{21}$$

If the unilateral effect is considered, the damage tensor can be defined as follows

$$D_{ijkl}=D_{ijkl}(\hat{\boldsymbol{D}}),\ \text{where}\ \hat{\boldsymbol{D}}=(\boldsymbol{P}^{+}+\alpha_D\boldsymbol{P}^{-}):\boldsymbol{D}, \tag{22}$$

where

$$\boldsymbol{P}^{+}=\frac{1}{4}\sum_{m=1}^{3}\sum_{n=1}^{3}H(S_m)(\boldsymbol{n}^{(m)}\otimes\boldsymbol{n}^{(n)}+\boldsymbol{n}^{(n)}\otimes\boldsymbol{n}^{(m)})\ (\boldsymbol{n}^{(m)}\otimes\boldsymbol{n}^{(n)}+\boldsymbol{n}^{(n)}\otimes\boldsymbol{n}^{(m)})$$

$$\boldsymbol{P}^{-}=\frac{1}{4}\sum_{m=1}^{3}\sum_{n=1}^{3}H(-S_m)(\boldsymbol{n}^{(m)}\otimes\boldsymbol{n}^{(n)}+\boldsymbol{n}^{(n)}\otimes\boldsymbol{n}^{(m)})\ (\boldsymbol{n}^{(m)}\otimes\boldsymbol{n}^{(n)}+\boldsymbol{n}^{(n)}\otimes\boldsymbol{n}^{(m)}) \tag{23}$$

(see Peng, *et al.* 1997). $H(\cdot)$ is the Heaveside function and α_D is a material parameter reflecting the unilateral nature and the pattern of microdefects in the damaged material.

Similarly,

$$M_H=1-[H(\sigma_{kk})+\alpha_H H(-\sigma_{kk})]D_I \tag{24}$$

In the above the actual stress can be calculated by

$$\boldsymbol{s}=\boldsymbol{M}^{-1}:\boldsymbol{s},\ \sigma_{kk}=M_H{}^{-1}\sigma_{kk} \tag{25}$$

4. Application and verification

4.1. Specification of damage evolution

The damage evolution rule is specified as follows

$$dD_i=A_D\left[\frac{(1-D_{II})^{\gamma_D}\langle s_i\rangle}{R_D f_D}\right]^{n_D}dz_D+A_H\left[\frac{\left(1-\frac{1}{3}tr(\boldsymbol{D})\right)^{\gamma_H}\langle\sigma_{kk}\rangle}{R_H f_H'}\right]^{n_H}dz_H \tag{26}$$

in which

$$\langle s_i\rangle=\frac{1}{2}[s_i+(1+\lambda_D)|s_i|],\ (i=1,\ 2,\ 3);\ \langle\sigma_{kk}\rangle=\frac{1}{2}[\sigma_{kk}+(1+\lambda_H)|\sigma_{kk}|] \tag{27}$$

$$\lambda_D\begin{cases}=0, & \text{if } s_k\geq 0\\ \in[0,2], & \text{if } s_k<0\end{cases}\qquad \lambda_H\begin{cases}=0, & \text{if } \sigma_{kk}\geq 0\\ \in[0,2], & \text{if } \sigma_{kk}<0\end{cases} \tag{28}$$

$$R_D=\sum_{r=1}^{n}\frac{C_r}{\alpha_r},\ R_H=\sum_{r=1}^{m}\frac{E_r}{\alpha_H^{(r)}},\ D_{II}=\sqrt{\frac{1}{3}D_{ij}D_{ij}} \tag{29}$$

The proposed damage model is able to describe the unilateral nature, the pattern of micro-defects, the damage mechanism and the failure mode of the damaged materials by an appropriate choice of the material parameters α_D, α_H, λ_D and λ_H (see e.g., Peng, *et al.* 1997).

On the other hand, the dependence of concrete responses on hydrostatic stress is considered by introducing the following relation,

$$C_r(J_1)=C_r'p(J_1),\ a_r(J_1)=a_r'p(J_1),\ (r=0,\ 1,\ \ldots,\ n) \tag{30}$$

where C_r and a_r are assumed to vary with respect to J_1 by the same rule so that α_r will be independent of J_1 (see Eq. (6)).

Following the procedure proposed by Peng, *et al.* (1997), one can determine the material parameters and constants in the present model.

4.2. Analysis for the response of concrete under triaxial loading case

The proposed damage model is applied to the analysis of the behavior of concrete subjected to triaxial loading and verified by the experimental results obtained by Scavuzzo, *et al.* (1983). Assuming for the hardening functions f_D and f_H the following simplest form

$$f_D=1+\beta_D z_D,\qquad f_H=1+\beta_H z_H \tag{31}$$

the coupling parameter f_{DH} to be constant, and adopting the following $p(J_1)$ obtained by Scavuzzo, *et al.* (1983),

$$p(J_1)=1-0.00932J_1-2.084*10^{-4}J_1^2\ \text{(MPa)} \tag{32}$$

and choosing $n=3$ and $m=1$, the material constants can be identified as:

$$E=42000\text{MPa},\ \nu=0.2,\ C_{1,2,3}'=16830,\ 560,\ 370,\ \alpha_{1,2,3}=12000,\ 447,\ 42.3,\ E_1=61200\text{MPa}$$
$$\alpha_H{}^1=320,\ \lambda_D=1.5,\ A_D=403,\ \beta_D=20,\ \lambda_H=0,\ \beta_H=15,\ n_D=2,\ \alpha_D=0.5,\ \gamma_D=0.5,\ f_{DH}=1.8 \tag{33}$$

where A_H and n_H is not necessary to be given for negative volumetric stress if $\lambda_H=0$ (see Eqs. (26) and (27)).

Fig. 2 shows the responses of the concrete specimens subjected to the deviatoric stress under hydrostatic pressure 56.3 MPa (8 ksi). The specimens were loaded monotonically or cyclically in stress space along the hydrostatic axis with gradually varying stress up to 56.3 MPa (8 ksi) followed by deviatorically varying stress paths denoted by TC, SS and TE without any change in the existing volumetric stress. Path designators TC, SS and TE stand for uniaxially compressive, purely shear and uniaxially tensile cyclic load path in the deviatoric stress plane, respectively (Scavuzzo, *et al.* 1983). The horizontal axis represents the three strain components, and the vertical axis the stress component with maximum absolute value. The stress histories in the three directions and the corresponding stress-strain curves are marked by *X*, *Y* and *Z*, respectively.

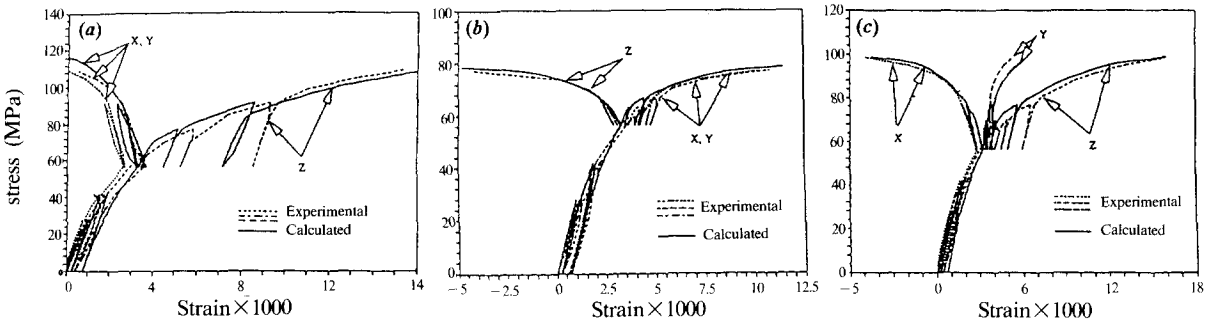

Fig. 2 Responses of concrete under hydrostatically cyclic stress paths followed by different paths at 56.3 (8 ksi) deviatoric stress plane.
(a) path TC; (b) path TE; (c) path SS

Fig. 2(a) shows the results for load path TC. Nonlinear volumetric deformation is observed as hydrostatic stress increases and under load cycling. When stress varies within the fixed deviatoric stress plane, it is observed that the experimental volumetric strain keeps developing in addition to the corresponding increment of deviatoric strain. In the direction where the sign of deviatoric stress coincides with that of hydrostatic stress, inelastic deformation increases faster. In other words, additional irreversible volumetric deformation occurs in the subsequent deformation process although there is no change in the hydrostatic stress. This kind of phenomenon (i.e., the shear-enhanced compaction under triaxial compression path) is well described by the present model.

The analytical and experimental results for load path TE under the hydrostatic stress of 56.3 MPa are shown in Fig. 2(b). The same phenomenon is observed as for load path TC, although in the deviatoric stress plane the deformation had changed from axial compression to axial tension. It is seen in the unloading/reloading process that in the tensile direction the experimental unloading slope is less than the analytical one. This is probably due to the existence of macrocracks that increase the deformation in the tensile direction when tensile stresses are large.

The response of the concrete subjected to the stress history along load path SS under hydrostatic stress of 56.3MPa is shown in Fig. 2(c). Although tensile stress s_X and compressive stress s_Z vary by identical values in the fixed deviatoric plane, a marked difference in the corresponding strain increments can be observed. In direction Y there is no deviatoric stress, but strains develop in the compressive direction. This demonstrates the effect of inelastic deviatoric deformation on the volumetric response.

The model was also used to reproduce the results obtained experimentally by Sinha, *et al.* (1964) for strain-controlled or stress-controlled monotonic and cyclic loads. In Fig. 3(a) the dashed curves represent respectively the experimental response envelopes of 28.1 MPa (4 ksi) concrete (Sinha, *et al.* 1964), which nearly enclose our analytical results. The experimental and the calculated results for cyclic stress-controlled process are shown in Fig. 3(b) and (c), respectively. It is seen that in the cyclic process, inelastic strain accumulates in each cycle but with increasing rate as the cyclic deformation proceeds, and at last leads to the fracture of the material, although the applied stress is much smaller than maximal strength of the material. It is seen the calculated results are in reasonable agreement with the experimental ones (see Sinha, *et al.* 1964).

It should be pointed out that, for the results shown in Fig. 3, generally, in the vicinity of the peak, the deformation ceases to be homogeneous and the data are more properly interpreted

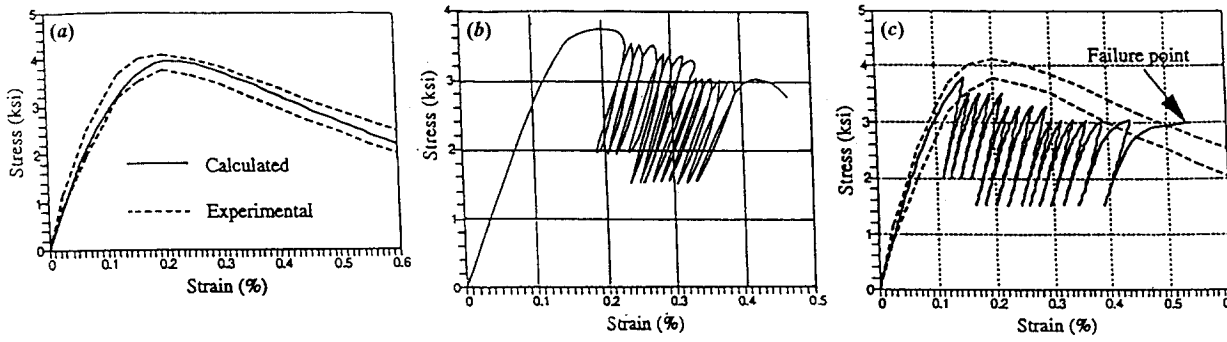

Fig. 3 Stress-strain curves of 4000 psi concrete subjected to monotonic compression and uniaxially cyclic stress history. (a) Monotonic compression, (b) Cyclic compression (experimental), (c) Cyclic compression (calculated).

as load-deflection data, so it might be more appropriate to consider a specimen as a structure, the resulting deformation field of which could be analyzed by the corresponding computational code. On the other hand, it was also pointed out that macrocracks may develop soon after the peak stress (Sinha, *et al.* 1964). In the proposed damage model, it is assumed that the non-homogeneity of deformation and the macrocracks are smeared and homogenized, so it may still be valid in a phenomenological description for the material response in the vicinity of the peak and in the post-peak region.

4.3. Analysis for the response of short fiber reinforced concrete

The above constitutive relationship is also applied to the analysis of randomly distributed short fiber reinforced concrete under triaxial loading and compared with experimental results.

In the present work concrete containing small amounts of fibers is considered. Such small amounts of fibers have little effect on strength, but there is a large increase in ductility, toughness and energy dissipation capability. This mechanism can be phenomenologically described by assuming the damage to be related to the fiber volume fraction V_f in the respective damage parameters (see Eq. (26)). Among these parameters γ_D and γ_H are found to be the most sensitive to V_f. Here we assume γ_D to take the following form

$$\gamma_D = \gamma_{D1} + (\gamma_{D2} + \gamma_{D3} J_1)\ V_f^{\gamma_{D4}} \tag{34}$$

where the dependence of γ_D on J_1 is considered due to the fact that the pull-out of fibers becomes more difficult at higher values of J_1. The form of γ_H can be determined in a similar way.

The experimental results obtained by Chern, *et al.* (1992) are used for the calibration of the material constants. The concrete consists of type I Portland cement, local crushed limestone aggregate with a maximum size 9.5mm (3/8 in.) and crushed fine aggregate. Steel fibers used were 19mm (3/4 in.) in length and 0.43mm (0.017 in.) in equivalent diameter, straight with a shallow notch on one side of each fiber. The concrete was designed for a 28-day strength of 20.65 MPa (3000 psi), with the weight ratios cement:fine aggregate:coarse aggregate:water = 1.00:1.50:2.50:0.58. The steel fiber content covers 0 (plain concrete), 1, and 2 percent of the volume of the mixture. The function $p(J_1)$ can be determined as follows by using the compressive failure

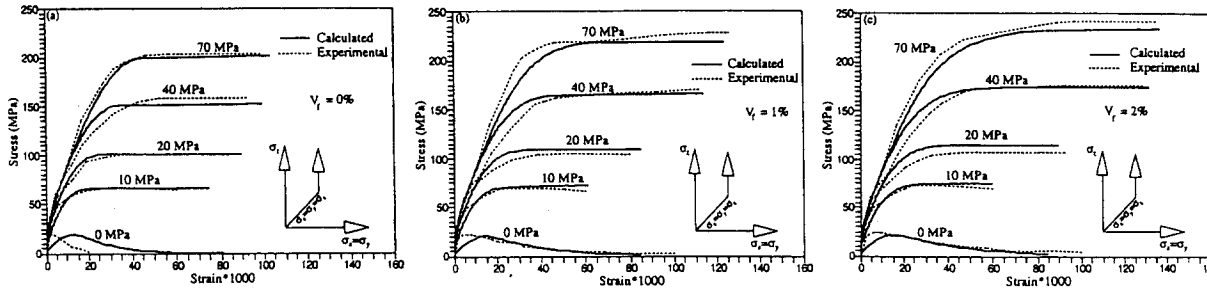

Fig. 4 Effect of confining pressure on σ_z-ε_z relations of concrete with different fiber contents. (a) V_f=0%; (b) V_f=1%; (c) V_f=2%

meridians of the plain concrete

$$p_c(J_1)=1-0.081J_1-10^{-4}J_1^2 \text{ (MPa)} \tag{35}$$

By choosing $n=3$ and $m=2$, the material constants are determined as:

$$\begin{aligned} &E=10375\text{MPa}, \quad \nu=0.35, \quad C_{1,2,3}'=6840,223,59, \quad \alpha_{1,2,3}=725,373,2.5, \\ &E_{1,2}=232000,5075\text{Mpa}, \quad \alpha_H^{1,2}=3750,50, \quad \lambda_D=1.0, \quad A_D=2600, \quad \beta_D=210, \quad \lambda_H=0, \\ &\beta_H=320, \quad n_D=1.2, \quad \alpha_D=1.0, \quad f_{DH}^{-1}=0, \quad \gamma_{D1,2,3,4}=0.5,1.71,0.012,0.5 \end{aligned} \tag{36}$$

Fig.4 shows the stress-strain relations in z-direction of plain and fiber reinforced concrete specimens under different confining pressures. In computation, the loading is stress-controlled when the confining pressure is non-zero (the load path is also shown in Fig. 4), otherwise the loading is strain-controlled so that the "softening" of the material can be described. It is seen that the strength of the concrete increases markedly as the confining pressure increases, while the increase of fiber volume fraction V_f slightly increases the material strength. A satisfactory agreement between the experimental and theoretical results is observed in a wide range of the confining pressure and fiber content. In the case of zero confining pressure, although differences between calculated and experimental results can be found, for fiber reinforced concrete the softening part of the curves is also well-described by the proposed model.

5. Conclusions

A comprehensive description of the damage of concrete was proposed and embedded in a thermomechanically consistent constitutive equation. This model takes into account the coupling between volumetric and deviatoric responses, which includes both the effect of hydrostatic stress on the inelastic deviatoric deformation and the additional inelastic volumetric deformation caused by inelastic deviatoric deformation (shear-enhanced compaction under triaxial compression path). A fourth-order damage effect tensor is introduced to describe both the anisotropic damage by assuming that damage develops in the principal directions of the effective stress, and the unilateral effect due to opening and closure of microcracks by introducing the projection tensors $\boldsymbol{P}^+$ and $\boldsymbol{P}^-$ determined by the current state of stress. The proposed damage model was applied to reproducing the response of plain and short fiber reinforced concrete subjected to complex loading histories and proved capable of describing the main characteristics of concrete.

References

ASCE Isenberg J. (editor, 1991). "Finite element analysis of reinforced concrete II", New York.
ASCE, Nilson A.H. (editor, 1982). "Finite element analysis of reinforced concrete", New York, 1982.
Chaboche, J.L. and Rousselier, G. (1983). "On the plastic and viscoplastic constitutive equations", *ASME, J. Pressure Vessel Tech.,* **105**, 153-164.
Chaboche, J.L. (1986). "Time-independent constitutive theories for cyclic plasticity", *Int. J. Plasticity,* **2**, 149-188.
Chern, J.C., Yang, H.J. and Chen, H.W. (1992). "Behavior of steel fiber reinforced concrete in multiaxial loading", *ACI Material Journal,* **89**, 32-40.
Fan, J. and Peng, X. (1991). "A physically based constitutive description for nonproportional cyclic plasticity", *J. Engng Mat. Tech.,* **113**, 254-262.
Fang, L. (1996). "Low-cycle fatigue behavior and damage mechanics of fiber reinforced concrete under biaxial stress states", PhD Dissertation, Columbia University, New York.
Lemaitre, J. (1984). "How to use damage mechanics", *Nucl. Engng. Des,* **80**, 233-245.
Paskova, T. (1994). "Low-cycle fatigue and damage mechanics of concrete with and without fiber reinforcement", PhD Dissertation, Columbia University, New York.
Peng, X., Fan, J. and Zeng, X. (1996). "Analysis for plastic buckling of thin-walled cylinders via nonclassical constitutive theory of plasticity", *Int. J. Solids Struct.,* **33**, 4495-4509.
Peng, X., Meyer, C. and Fang, L. (1997). "Thermomechanically consistent damage model for concrete materials", *J. Engng. Mech.,* **123**, 60-69.
Peng, X. and Ponter, A.R.S. (1994). "A constitutive law for a class of two-phase materials with experimental verification", *Int. J. Solids Struct.,* **31**, 1099-1111.
Scavuzzo, R., *et al.* (1983). "Stress-strain curves for concrete under multiaxial load histories", *Report to National Science Foundation*, Department of Civil, Environmental, and Architectural Engineering, University of Colorado, Boulder.
Sinha, B.P., *et al.* (1964). "Stress-strain relations for concrete under cyclic loading", *ACI Journal, Proceedings,* **61**(2), 195-211.
Valanis, K.C. (1980) "Fundamental consequences of new intrinsic time measure plasticity as a limit of the endochronic theory", *Arch. Mech.,* **23**, 171-190.
Watanabe, O. and Atluri, S.N. (1986). "Internal time, general internal variable and multi-yield surface theories of plasticity and creep: A unification of concept." *Int. J. Plasticity,* **2**, 37-52.

Notations

The following symbols are used in this paper:

$\boldsymbol{a}_r$, $\bar{\boldsymbol{a}}_r$ = initial and damaged damping coefficients of the rth dashpot-like block, respectively
a_r = rth scalar damping coefficient
b_r = rth volumetric damping coefficient
C_r = initial stiffness coefficient of the rth spring
c_r, $\bar{c}_r$ = fourth-order initial and damaged stiffness tensors of the rth spring
$\boldsymbol{D}$, $\boldsymbol{D}$ = second order damage tensor and fourth order damage tensor
D_I, D_{II} = first and second invariances of $\boldsymbol{D}$
$\boldsymbol{D}$ = damage tensor taking into account unilateral effect
E_r = rth initial volumetric stiffness coefficient
$\boldsymbol{e}^i$, $\boldsymbol{e}^e$, $\boldsymbol{e}$ = inelastic, elastic and total deviatoric strain tensors, respectively
f_D, f_H' = deviatoric and volumetric hardening functions, respectively
f_{DH} = coupling parameter taking into account shear-enhanced compaction
J_1 = first invariance of stress tensor

K, $\bar{K}$ = initial and damaged elastic volumetric modulus
$\boldsymbol{M}$, M_H = damage effect tensor and volumetric damage effect variable, respectively
$\boldsymbol{n}^{(k)}$ = kth eigenvactor of a second order tensor
$\boldsymbol{P}^+$, P^- = projection operators
$p(J_1)$ = parameter taking into account the hydrostatic pressure on deviatoric response
$p^{(r)}$ = rth deviatoric internal variable
$\boldsymbol{Q}^{(r)}$ = rth generalized frictional force
S, $\bar{S}$ = deviatoric stress tensor and effective deviatoric stress tensor
z_D, z_H = generalized time for inelastic deviatoric and volumetric strain histories, respectively
α_D, α_H = material parameter reflecting the unilateral effect on deviatoric and volumetric response, respectively
α_r = C_r/a_r, fading memory coefficient for the rth deviatoric dissipative mechanism
$\alpha_H{}^{(r)}$ = fading memory coefficient for the rth volumetric dissipative mechanism
β_D, β_H = deviatoric and volumetric hardening parameters, respectively
ζ_D, ζ_H = generalized time measures for inelastic deviatoric and volumetric strain histories, respectively
λ_D, λ_H = material parameters reflecting, respectively, the deviatoric and volumetric stress states on damage
$\bar{\boldsymbol{u}}$, u = the fourth order damaged elastic shear modulus tensor and initial elastic shear modulus
σ_{kk}, $\sigma_{kk}{}^{(r)}$ = volumetric stress and its rth component
$\bar{\sigma}_{kk}$ = effective volumetric stress
$\varepsilon^i{}_{kk}$, $\varepsilon^e{}_{kk}$, ε_{kk} = inelastic, elastic and total volumetric strain, respectively